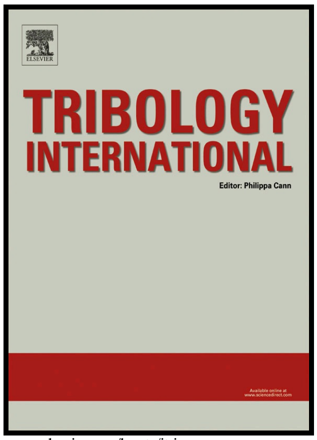

www.elsevier.com/locate/jtri

Multiscale analysis of the effect of roughness on fretting wear

K. Pereira, T. Yue, M. Abdel Wahab

PII: S0301-679X(17)30084-1
DOI: http://dx.doi.org/10.1016/j.triboint.2017.02.024
Reference: JTRI4605

To appear in: *Tribiology International*

Received date: 9 December 2016
Revised date: 14 February 2017
Accepted date: 17 February 2017

Cite this article as: K. Pereira, T. Yue and M. Abdel Wahab, Multiscale analysis of the effect of roughness on fretting wear, *Tribiology Internationa* http://dx.doi.org/10.1016/j.triboint.2017.02.024

Multiscale analysis of the effect of roughness on fretting wear

K. Pereira[1], T. Yue[1], M. Abdel Wahab[2,3,4,*]

[1]Department of Electrical Energy, Systems and Automation, Faculty of Engineering and Architecture, Ghent University

[2]Division of Computational Mechanics, Ton Duc Thang University, Ho Chi Minh City, Vietnam

[3]Faculty of Civil Engineering, Ton Duc Thang University, Ho Chi Minh City, Vietnam

[4]Soete Laboratory, Faculty of Engineering and Architecture, Ghent University, Technologiepark Zwijnaarde 903, Zwijnaarde B-9052, Belgium

*****Correspondence: magd.abdelwahab@tdt.edu.vn; magd.abdelwahab@ugent.be

Abstract: Fretting occurs when two loaded contacting surfaces are exposed to oscillatory relative movement of small amplitude. Depending on conditions such as surface finishing, coefficient of friction, normal load and slip amplitude, fretting may reduce the service life of a component by fretting wear. The effect of surface roughness on the fretting wear profile is still uncertain and may be significant. However, most of the finite element (FE) models that are used to predict fretting wear do not take it into consideration. In this paper, we propose a multiscale procedure to study roughness effect on fretting wear using FE models. In order to do that, we treat the problem in two scales: a) micro scale to analyse the effect of roughness on the contact pressure for frictionless conditions, and b) macro scale to estimate the wear profile evolution for a cylinder on plane contact configuration.

Keywords: Multiscale analysis, Finite element analysis, Fretting wear, Roughness

1 Introduction

Fretting happens when two contacting surfaces, normally loaded, are submitted to small oscillatory relative movement. It may lead to catastrophic failure of many mechanical components due to fatigue (known as fretting fatigue), or it may produce loss of fitting due to wear (fretting wear) or even a combination of both.

Among these failure mechanisms, wear is a complex material damage process involved in many research areas such as contact mechanics, friction and material science. Understanding the engineered contact surface, where asperities are statistically distributed, is very important for studying these research topics [1], in particular fretting wear [2, 3].

However, the effect of roughness on wear and frictional response is still uncertain and a brief literature review shows that there are even conflicted conclusions to the problem. On one hand, some studies [4] showed that roughness has a considerable impact on friction characteristics and should, therefore, be taken into consideration. On the other hand, some defend that its effect is negligible [5]. For fretting conditions, experimental results presented by Kubiak and Mathia [6] and Kubiak et al. [7, 8] showed that roughness has a strong influence on the fretting regime and also on the amount of wear for both lubricated boundary and dry metallic (steel/steel) fretted bodies. Although their findings indicated that surface asperities impacts the amount of wear under gross slip conditions, other researchers found opposite results [9, 10].

Besides investigating fretting damage by experiments, Finite Element Method (FEM) is also widely used in this field in partial slip [11-17] and gross sliding [18] regimes. The first FEM of fretting wear presented in 2004 [19]. The advantage of FEM is that it can describe the local contact information and fretting damage during the fretting wear process, which is difficult to achieve by experiment. However, most of the models that are used to predict fretting wear do not consider the effect of roughness [18-20] due to the small size of asperities and its statistical distribution leading to high computational demanding. Though the semi-analytical model proposed by Kasarekar et al. [21] and the discrete element approach study done by Leonard et al. [22] simulated the effects of roughness on fretting wear, both of them only neglected the random nature of the rough surfaces, analysing only one roughness profile per case. Kasarekar et al. [21] only analysed wear evolution under partial slip conditions and, here we are interested in results under gross sliding conditions. Although Leonard et al. [22] presented results for those conditions, their numerically generated surfaces were constructed considering only one roughness parameter (R_q), neglecting the effect of the horizontal distribution of asperities, this will be considered in the present work.

In order to obtain abundant fine mesh at asperities and increase computational efficiency, the asperity model should be scaled down to a micro model and techniques that allow this small scale model to be incorporated in the macro fretting wear model are of great interest. In this regard, multiscale modelling offers the advantage to efficiently connect results from different scales and being thus a powerful tool to deal with roughness in fretting. Aboudi et al. [23] classify multiscale techniques in three main groups: hierarchical, concurrent and semi-concurrent. Different from the other approaches, concurrent technique is a fully coupled methodology, which means that all scales are handled at once in the same numerical model. Recent work has been done using this technique applied to account for roughness effect on contact problems [24-26], nevertheless none of them considered the impact of surface asperities on fretting conditions.

The hierarchical method has the advantage of requiring low computational costs and providing relatively good accuracy, being, therefore, able to incorporate many complex physical phenomena in the simulations. It has been used for analysing many contact problems, as elucidated by Stupkiewicz et al. [27]. For instance, Temizer and Wriggers [28] studied inelastic contact considering effect of third bodies and also friction of soft matter [29]. Jerier and Molinari [30] presented a methodology to analyse the non-adhesive and frictionless contact between a flat elastic body and a rigid surface with fractal roughness. Although many work has been done in hierarchical analysis of contact phenomena, most of them proposed macroscopic constitutive relations for the contact stiffness based on microscopic simulations and were not applied to fretting problems.

The main goal of this paper is to present a sequential multiscale approach, which is capable to consider the effects of roughness in FE analysis of fretting under gross sliding conditions. In our proposed approach the surface roughness is numerically generated, considering the asperities distribution in horizontal and vertical directions. Also, here a set of rough surfaces were analysed and a statistical analysis was done to account for the random nature of rough surfaces. We will consider two independent contact models: a micro scale model containing the roughness geometric details and a macro scale model of the fretting wear problem. A multiscale procedure together with a statistical analysis will be used to link the average response of the micro model to the macro model. Therefore, scale separation for the normal contact behaviour is assumed here.

The paper is organized in the following way. Before exploring the micro scale model, a brief description of the approach for numerically generating rough surfaces is done in section 2. Then, the micro scale FE models used to study the normal frictionless contact of rough bodies together with the two-dimensional (2D) macro model used to simulate fretting condition are introduced in section 3. Finally, in section 4, the results are discussed and compared against experimental data and the main conclusions are presented in a separated section.

2 Numerical generation of random rough surfaces

For the real engineered surfaces, both the radius and the heights of the surface irregularities have a statistically distribution. Naylor [31] developed a method to generate random roughness using only the statistical properties of real surfaces, which are asperities height distribution and asperities height correlation function. In this paper, an improved approach presented by Hu and Tonder [32] based on [31] is employed, using digital filter techniques (spectrum analysis and Fourier transform) to generate random surfaces with Gaussian auto-correlation functions.

In order to generate the random rough profile, two parameters are defined: the root mean square (RMS) of the surface roughness R_q and correlation length ξ. They are statistical parameters calculated from real surfaces measurements. The parameter R_q can easily be measured in laboratory. For a 2D profile, it can be calculated as:

$$R_q = \sqrt{\frac{1}{l}\int_0^l Z(x)^2 dx} \tag{1}$$

where l is a pre-set sampling length and $Z(x)$ is the measured profile from the profilometer. The parameter ξ is the length at which the auto-correlation function reduces to 10% of its value at origin. It is related to how the asperities are distributed horizontally. Figure 1 illustrates how these parameters change the shape of the asperities and, therefore, the roughness profile. The R_q clearly affects the amplitude of the profile, while the ξ alters the horizontal distribution of the asperities.

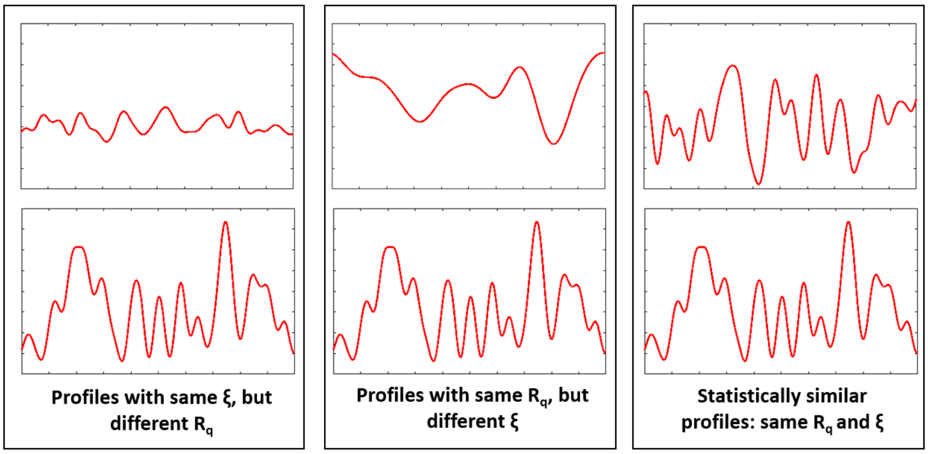

Figure 1. Different simulated profiles showing the necessity of at least two parameters to statistically define the 2D roughness

The roughness profiles were numerically simulated using a code written in Matlab® to generate coordinates (*x*,*y*) of a 2D rough profile used in FEM. Aiming to validate the methodology presented above, the simulated profiles is compared with mill finished aluminium surface measured by a Surfascan 3D stylus as shown in Figure 2. It is important to notice that using this approach, the generated profiles are all statistically identical to the profile measured in the laboratory.

3 FE model description

3.1 Micro models: Roughness effect on normal load

In order to quantify the roughness effect on the contact pressure distribution, we analysed the interaction between the fretting pad and specimen using a micro scale model, which consists of a small part of the larger model containing the entire contact region (see Figure 3 for more details). A FE analysis was performed in ABAQUS® considering the bodies, part of the cylinder and part of the plane, with numerically generated roughness profiles created using a Matlab® code. Here, as a first approximation, we are only interested in how the roughness affects the contact pressure distribution at interface, considering only normal frictionless contact between the bodies.

As we would like to validated the wear scar obtained via FEM with experiment data by McColl et al. [19], both parts of the FE model had the same material properties as in [19], which is presented in Table 1. An elastic-perfectly plastic material response was considered in this study.

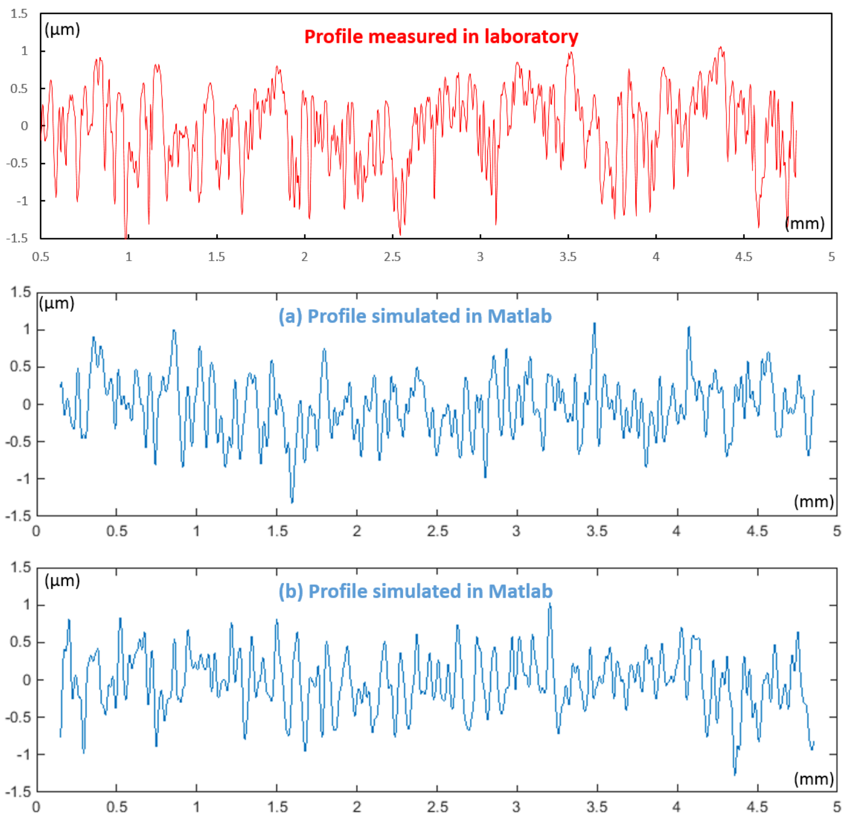

Figure 2. Comparison between two numerical generated random roughness profiles (a) and (b) and a profile measured in laboratory (R_q = 0.4µm and ξ = 25µm)

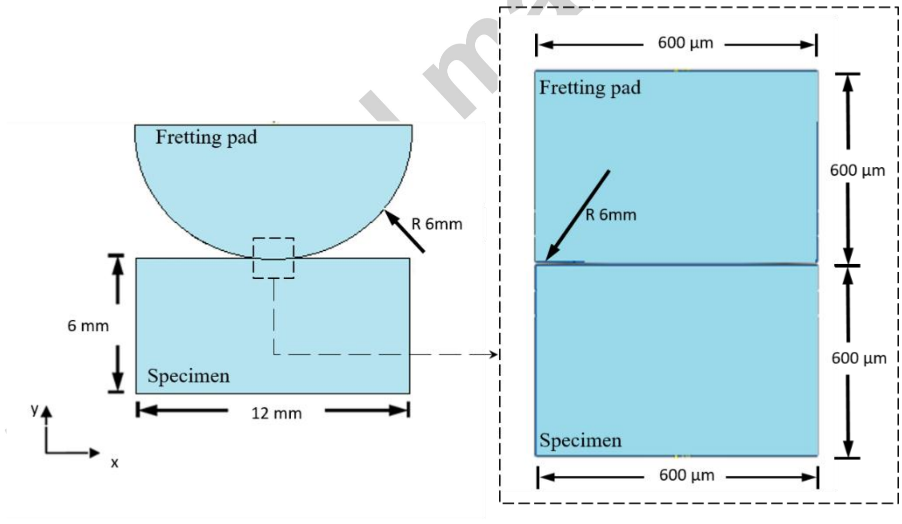

(a) (b)

Figure 3. (a) Dimensions of macro fretting wear model; (b) Details of micro models and their dimensions

Table 1. Material properties for Super CMV steel (data from McColl et al. [19])

E	Modulus of Elasticity [GPa]	200
ν	Poisson's ratio	0.3

$\sigma_{0.2}$	Yield Strength [MPa]	1240

A Python script was created to import the rough profile coordinates from Matlab® into the ABAQUS FE model. These coordinates were later fitted using a spline curve, in order to generate the contacting surfaces of the two rough bodies (specimen and pad). The FE mesh with the boundary conditions and the applied load are depicted in Figure 4. Regarding the mesh details, a 2D quadrilateral, 4-node (bilinear), plane strain, reduced integration element (CPER4) was used and the mesh size of 0.25μm was considered at the contact interface and gradually raised as the distance from the contact region increased.

The bottom surface of the bottom specimen was fully fixed (restricted movement in the *x* and *y* directions and restricted rotation, i.e., $U_x = U_y = 0$ and $R_{xy} = 0$) and a vertical concentrated normal load *F* was applied to the reference point at the middle of the top surface of the pad. A Multi-Point Constraint (MPC) was used to constrain the degrees of freedom of a slave edge (top surface of the pad) according to the degrees of freedom of the master point (reference point in the middle of the top surface). Finally, the master-slave algorithm in ABAQUS® was used to define the contact interaction between the parts, Lagrange multiplier formulation was used to define the tangential behaviour and a hard contact approach was used to define the normal behaviour of the contact pair.

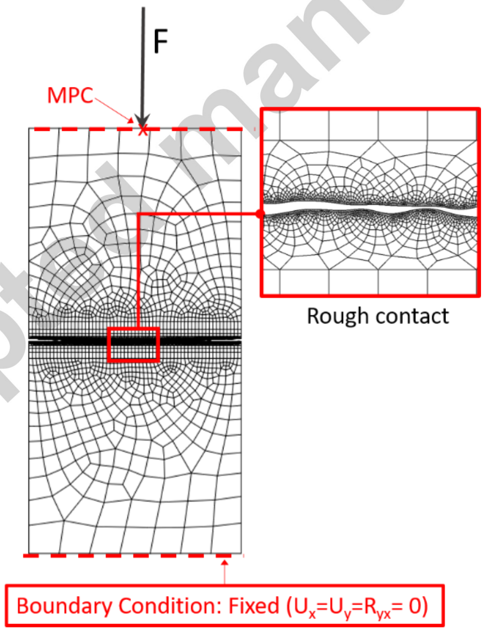

Figure 4. Micro fretting model with roughness

In order to consider the randomness effect of the roughness on normal load, a large number *n* of micro models (*n* = 50) were created, each one with a different pair of roughness profiles, but with the same statistical properties R_q and ξ. Each model was subjected to a normal load *F* in a single step and the contact pressure distribution along the interface was then calculated considering a frictionless contact interaction. Three different values of *F* were considered:

185 N, 500 N, 1670 N (same as the ones imposed on experiments done by McColl et al. [19]). The final average contact pressure distribution at the interface was then obtained by averaging the nodal contact pressure results from all *n* rough contact models for each case of normal load *F*.

For the multiscale analysis presented in this paper, the parameters R_q and ξ were chosen based on the measurements of real steel surfaces presented by Singh et al. [4] and are reproduced here in Table 2. As it can be seen in Figure 5, the isotropic and grounded surfaces have very different roughness profiles, being the grounded one considerably more rough than the isotropic. Analysing both types of surfaces finishing allowed as to study the influence of increasing roughness in our results.

Table 2. Roughness parameters for different types of surface [4].

Type of surface	*Rq* [μm]	ξ [μm]
Isotropic	0.083	20.0
Grounded	0.424	5.5

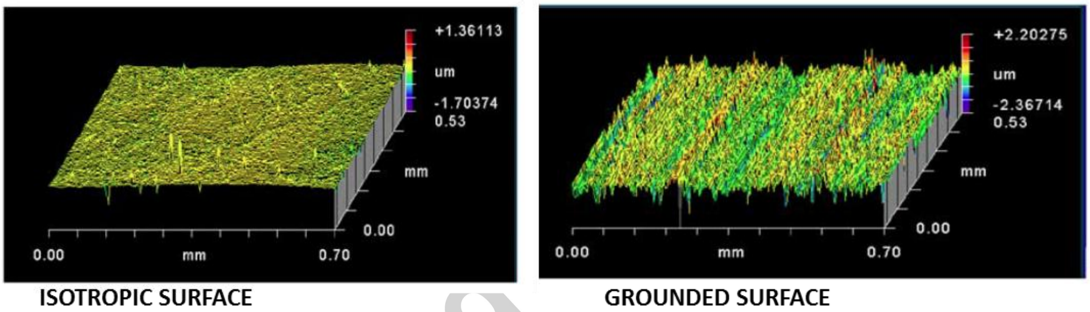

Figure 5. Types of surfaces (from Singh et al. [4]).

3.2 From micro model to macro model

In this work, we are interested in the effects of micro scale surface features on the macro scale fretting problem. The multiscale methodology can be used to bridge information between models of these two different scales. It can be used as a one-way approach, i.e., the analysis of the micro model is done independently of the model performed in the macro analysis. In this scenario, the average response of a small scale can be used as input for the large scale model, or vice-versa.

Here the focus is in a sequential methodology capable of extracting the effect of surface roughness on the contact pressure distribution, providing an average response at small scale that could be up-scaled to a macro model. The impact of the presence of roughness on the contact pressure distribution can be observed in the results section 4, where the FE results are compared with the Hertzian distribution [33]. However, for illustration purposes, the results for an isotropic surface for the loading *F*=185 N are shown at Figure 6. The dashed line represents the analytical Hertzian contact pressure obtained considering contact of two smooth surfaces, the solid grey line is the solution obtained by the micro scale FE analysis considering the contact of rough bodies. Comparing these two curves, it can be seen that the presence of asperities changes the distribution of the contact pressure considerably. In addition, the contact pressure distribution obtained from micro models is not a smooth curve, causing difficulties to import it directly in the macro-scale model. This section describes how results calculated from micro model were integrated to macro models.

The first step was to generate an approximated function that captured the important features of the micro scale solution, making it possible to link the results from micro to macro scale models. In order to do that, the contact pressure obtained by the FE analysis was smoothed (solid red curve in Figure 6) using a kernel smoothing procedure, available as a package in the statistical software R. The kernel smoothing provides a weighted average of the data of interest within a smoothing window [34], defined by a fixed parameter known as the bandwidth *b*. As also shown in Figure 6, based on the smoothen curve, we can extract two main parameters: the peak average pressure p_{max} and the effective contact width a_{micro}. The peak average pressure was used to adjust the geometry of the macro model as explained in the following. The smoothened curve results for different types of surface roughness and loading conditions are presented in section 4.

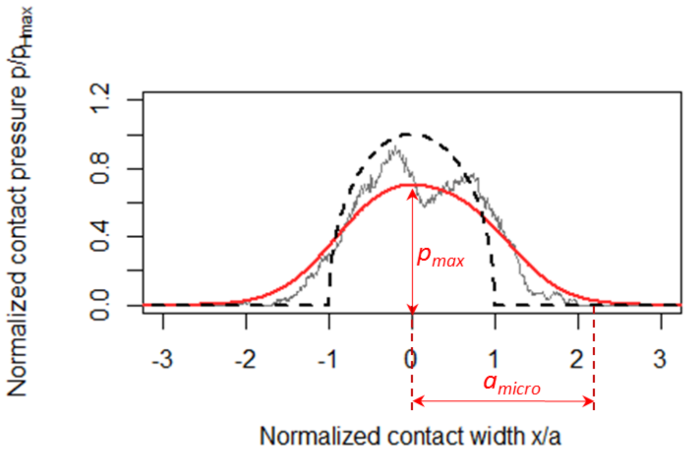

Figure 6. Normalized contact pressure distribution for an isotropic surface, F = 185 N, a = 35.86 µm, p_{Hmax} = 328.4 MPa, a_{micro} = 0.072 mm and p_{max} = 229.88 MPa

Aiming to obtain a contact pressure distribution at macro scale as similar as possible to the one calculated at micro scale considering roughness, the equivalent radius of the pad of the macro model R_E was modified based on the results in the micro model and Hertzian solution. Indeed, the smoothened contact pressure distribution provides both the contact maximum pressure p_{max} and the contact width a_{micro}, which give two various radii of the pad according to equations (2) and (3), respectively.

$$R_{Ep} = \frac{FE^*}{\pi {p_{max}}^2} \quad (2)$$

$$R_{Ea} = a_{micro}{}^2 \frac{E^*\pi}{4} \quad (3)$$

where $\frac{1}{E^*} = \frac{1-\upsilon_1{}^2}{E_1} + \frac{1-\upsilon_2{}^2}{E_2}$, E_1 and E_2 are Young' modulus, and υ_1 and υ_2 are Poisson's ratios of each contact body.

The chosen value of R_E should lead to the approximate contact pressure distribution obtained by the micro scale analysis in the macro model. Therefore, we have not used the value of a_{micro} to adjust the geometry of the macro model, but R_E was calculated based on p_{max}. This choice was driven by the fact that the distribution of contact pressure with R_{Ep} is closer to the smoothened curve than the case of R_{Ea}, as illustrated in Figure 7.

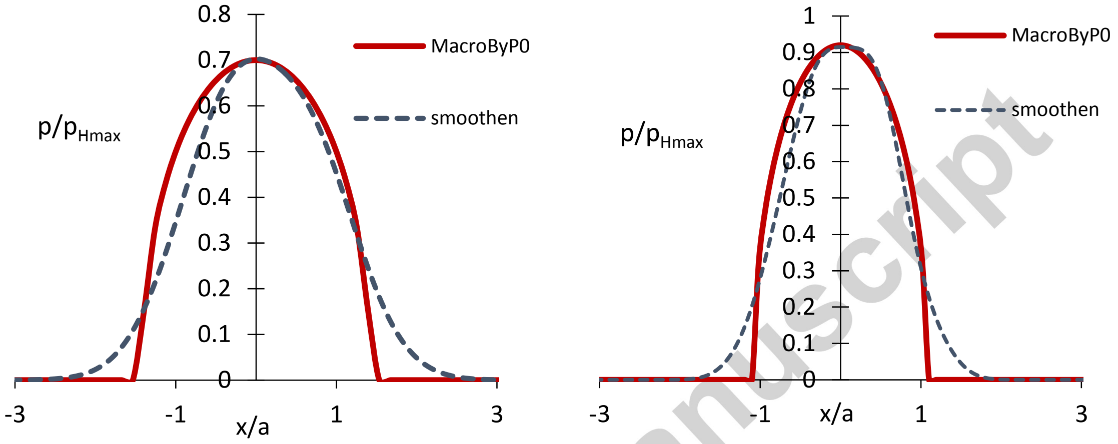

Figure 7. Contact pressure distribution obtained by kernel smoothening and by changing the pad radius for R_{Ep}

As explained in the study on fretting wear of steel [35], at the running-in stage of the coefficient of friction (CoF) evolution, the contact surface of steel is progressively roughened due to fretting wear. Meanwhile, the surface separation due to the debris generation could reduce CoF. With the progress of fretting wear, the interaction of the increased roughening and increased separation of contact surfaces may lead to a dynamic equilibrium when CoF shows constant. Therefore, the effects of roughness were considered in running-in stage (3000 cycles) by using the equivalent radius of the cylinder with R_{Ep}. It means the initial radius of the cylinder was R_{Ep} and it was modified back to the original value equalling to 6 mm, which was used for the experiment, after 3000 cycles. R_{Ep} of different normal load cases is listed in Table 3.

Table 3. R_{Ep} used for the running-in stage in various loading cases

F [N]	R_{Ep} [mm] for isotropic surface	R_{Ep} [mm] for grounded surface
185	12.25	28.36
500	7.08	14.20

1670	-	8.71

3.3 Macro model: Fretting wear prediction

The macro model used in this study is similar to the one proposed by Yue and Wahab [18] based on McColl et al. [19]. The contact configuration with dimensions is shown in Figure 8, where the normal load *F* and the tangential reciprocated displacement with amplitude *D* are imposed at the midpoint of the top surface. During the whole loading history, the bottom and side edges of the bottom specimen are completely constrained. At the first loading step, *F* is applied and only the vertical movement of the cylinder is allowed. Next, an oscillatory tangential displacement with amplitude of 25 μm is imposed during moving steps, i.e. 18000 cycles. In the end, the unloading step is applied for removing the elastic deformation in the contact surface caused by the normal load.

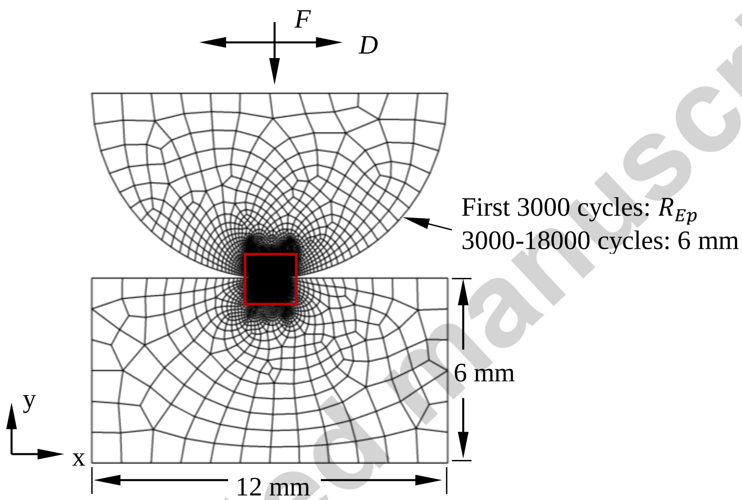

Figure 8. Contact configuration and dimensions of the macro fretting wear model

Energy method is utilized as the wear model for simulating the process of fretting wear and the following inputs were adopted in the simulations. In all cases of this study, each moving step was analysed in 100 increments and the jump cycle was chosen equal to 1000 to reduce computation time. The material properties of the macro model is the same as those of the micro model. In addition, the definition of the contact interaction is based on master-slave technique, in which the contact surface of cylinder is master surface and the other surface of contact is slave surface. The CoF and wear coefficient α_h in three loading conditions are listed in Table 4. Finally, the evolution of stress distribution and the wear scar due to fretting wear could be simulated by calling UMESHMOTION subroutine of ABAQUS® after every increment of each moving step.

Table 4. CoF and α_h used in fretting wear simulations

F [N]	CoF	α_h [$\times 10^{-8}$MPa^{-1}]
185	0.88	3.33
500	0.75	7.33
1670	0.6	4.41

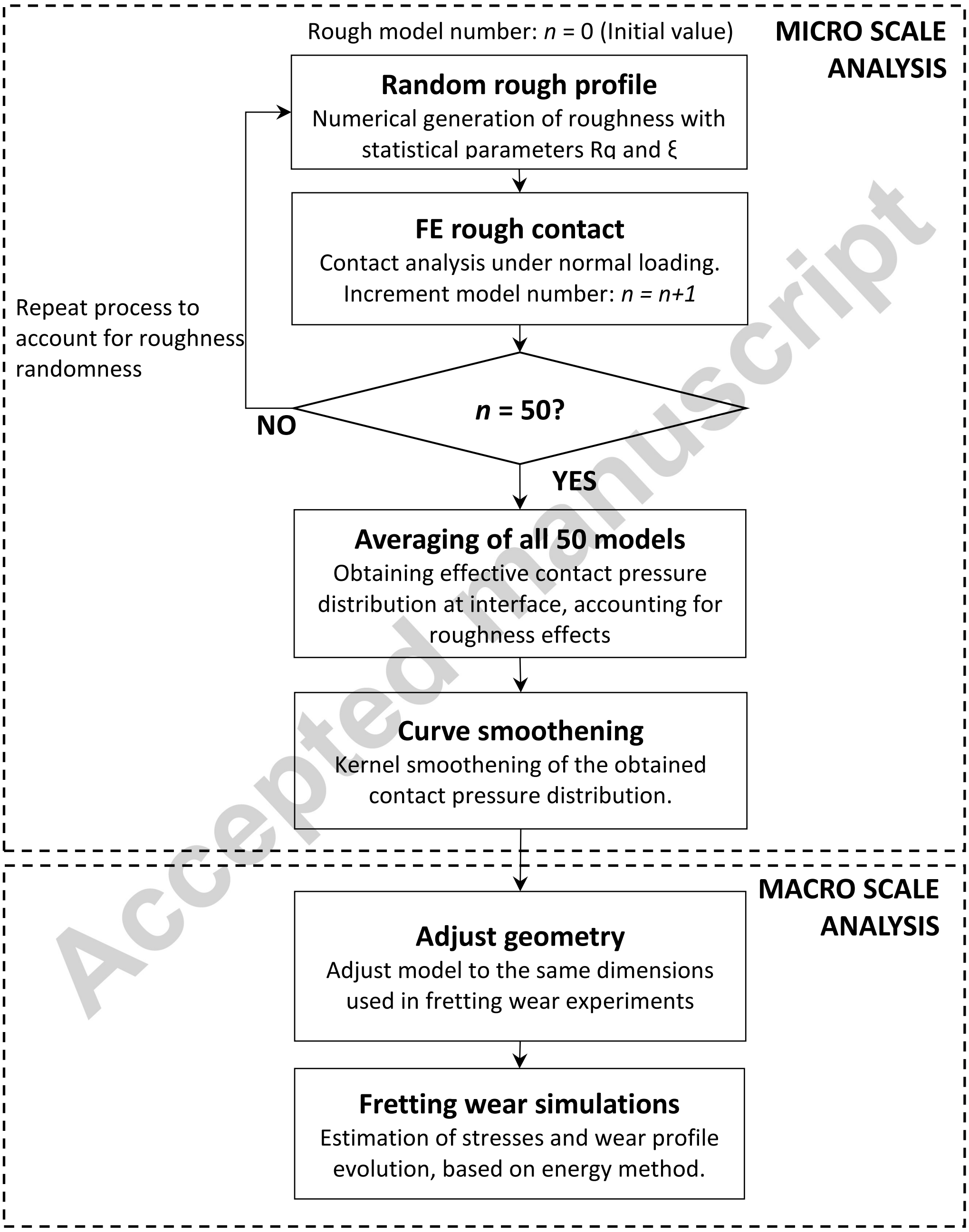

Figure 9. Flow chart of the multiscale approach

4 Results and Discussions

4.1 Roughness effect on normal load

We started our micro scale analysis with normal frictionless contact of two smooth surfaces, i.e., without any roughness. We used the procedure described in section 2 to generate the coordinates for the two bodies and by setting the roughness parameters R_q and ξ to zero, we created smooth surfaces at the cylindrical pad and flat specimen. In order to verify the response of this micro model and also to check the applied boundary conditions, we applied the three cases of normal contact load F to the model and calculated the contact pressure distribution along the interface. The results were compared with analytical Hertzian solutions [33] and are presented in Figure 10. The curves were normalized using Hertzian contact width a and maximum contact pressure p_{Hmax} to facilitate a visual comparison. Notice that the solution from the micro scale smooth FE model is in good agreement with the normalized analytical solution (differences are less than 5%), which suggests that the dimensions and boundary conditions used on the analysis of the micro models are suitable.

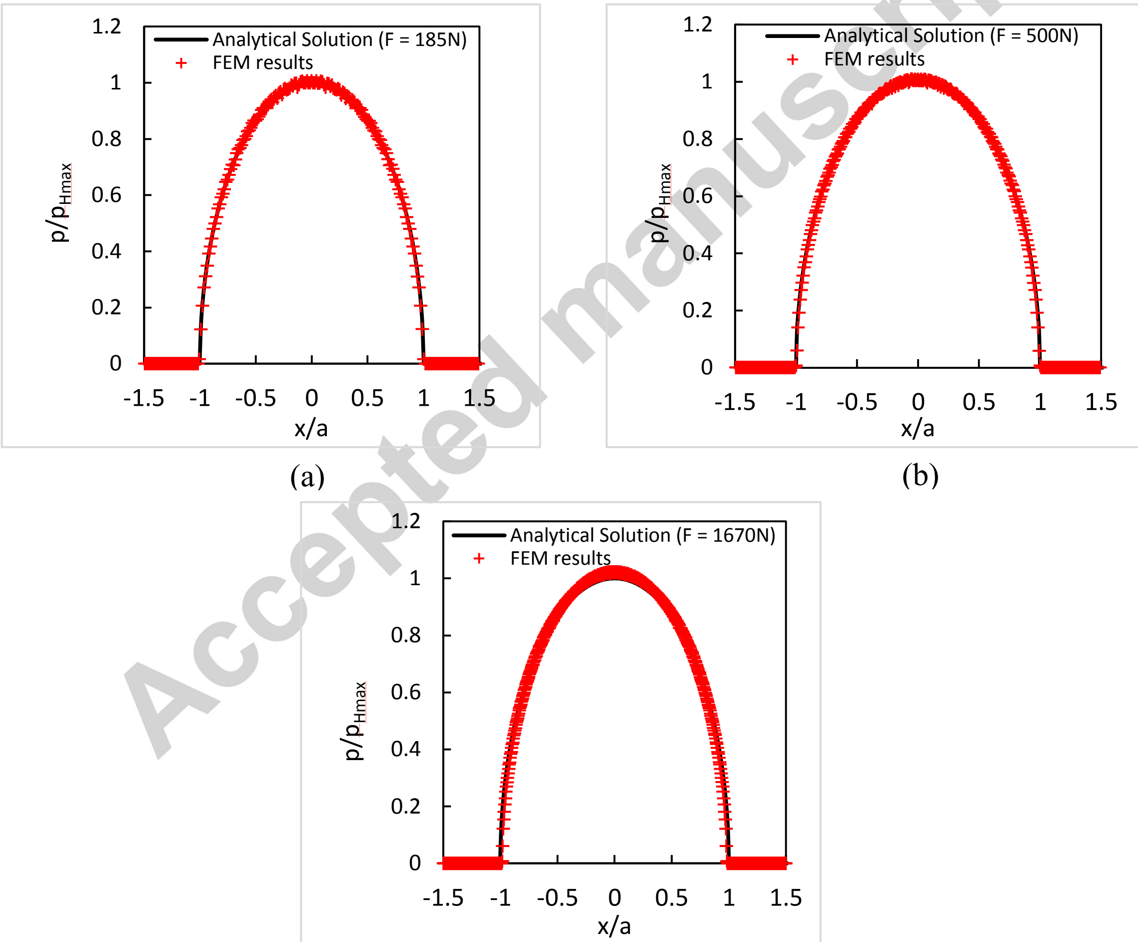

(a) (b) (c)

Figure 10. Comparison between micro-model (without any roughness) and Hertzian analytical solutions for the three cases of normal loading F analysed in this study: (a) F = 185N, a = 35.86 µm, p_{Hmax} = 328.4 MPa; (b) F = 500 N, a = 58.96 µm, p_{Hmax} = 539.9 MPa; (c) F = 1670 N, a = 107.75 µm, p_{Hmax} = 986.7 MPa.

The micro models were then used to estimate the effect of roughness under normal loading conditions. The effective contact pressure, obtained by the analysis of the 50 rough contact models, for each loading F considering an isotropic surface is presented in Figure 11 and considering a grounded surface is presented in Figure 12. The grey curves are the FE analysis results, the dashed black lines are the Hertzian analytical solutions and the red curves are the kernel smoothed results. The value of bandwidth b used in each kernel smoothing procedure as well as the values of p_{max} and a_{micro} are also presented in those figures.

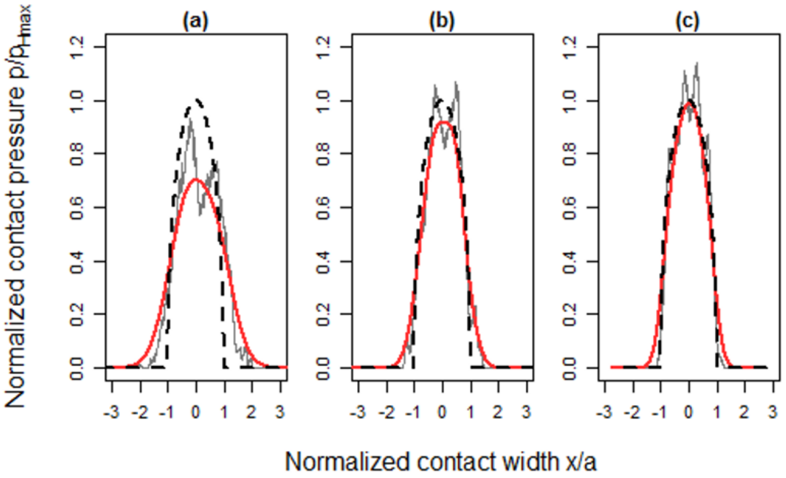

Figure 11. Micro-model results for isotropic surface: (a) F = 185N, a_{micro} = 100.0µm, p_{max} = 230.7MPa and b = 0.45; (b) F = 500N, a_{micro} = 115.5µm, p_{max} = 494.1MPa and b =0.25; (c) F = 1670N, a_{micro} = 185.6µm, p_{max} = 975.8MPa and b = 0.25.

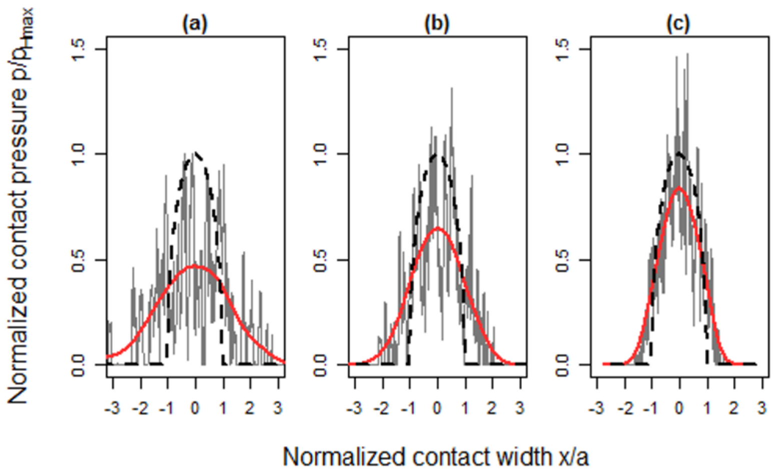

Figure 12. Micro-model results for grounded surface: F = 185 N, a_{micro} = 151.7 µm, p_{max} = 152.9 MPa and b = 0.5; (b) F = 500 N, a_{micro} = 175.8µm, p_{max} = 348.4 MPa and b =0.4; (c) F = 1670 N, a_{micro} = 234.5 µm, p_{max} = 827.2 MPa and b = 0.3.

Comparing the contact pressure distribution obtained by the FE analysis with the analytical Hertzian distribution, it is noticeable that the presence of asperities has a major impact on the shape of the distribution. For the same loading condition, comparing Figure 11 and Figure 12, it can be seen that, as the roughness of the surface increases (from isotropic to grounded), the peak of effective contact pressure p_{max} reduces and the apparent contact width a_{micro} increases. Hence, as the surface becomes rougher, the contact pressure distribution gets even further away from the analytical Hertzian distribution.

Another interesting point is that, for the same roughness, there is a dependency between the normal load and the effective peak pressure p_{max}. For higher values of normal load, the value of p_{max} gets closer to the analytical value of p_{Hmax}. Therefore, if the geometry and roughness parameters are kept constant, one can conclude that, for higher normal loads, the Hertzian analytical solution is a good approximation of the contact pressure.

Even though our analysis does not make an assumption of spherical shaped asperities, our results follow the same trend observed by Greenwood & Tripp [36]. As a general result, it can be said that Hertzian distribution is only an acceptable approximation for higher normal loads and relatively smooth surface (case (c) in Figure 11). Therefore, fretting wear under the case of higher normal load (F= 1670 N) with isotropic surface is not considered in the following fretting wear analysis.

4.2 Effects of roughness on fretting wear

As the effect of roughness is considered at the first 3000 cycles, using the equivalent radius R_{Ep} to reproduce the contact pressure distribution calculated from the micro scale, it is interesting to study the wear scars after this number of cycles. These wear scars are presented in Figure 13. In the lowest normal load case (F =185 N) of this work, increasing the roughness of the contact surface leads to wider wear width and less wear depth. However, in the higher normal load cases, wear width does not grow when the surface is rougher, however, the wear depth shows similar decreasing tendency as in the lower normal load case. Therefore, generally, the numerical results indicate that the FE model without considering roughness of the contact surface overestimates fretting wear depth at the running-in stage in the gross sliding condition.

During the running-in period, the surface asperities evolve changing the coefficient of friction and causing a dependence of the friction behaviour of the contact pair on the initial surface roughness. Hisakado et al. [37] observed that for higher initial values of roughness, a lower CoF is expected. As the wear volume is proportional to CoF, a lower instantaneous value of wear volume is obtained for higher values of roughness. An inline conclusion is also observed in our simulations when having a closer look at the wear volume after 3000 cycles in various contact surfaces, listed in Table 5. It is found that the fretting couple of grounded surface has the lowest wear volume in all normal loading cases.

These results presented in Figure 13 and also experimental evidence presented in [7] show that surface asperities interaction do have an impact on the wear scars, but only for the initial thousands cycles and should, therefore, be considered in order to improve the quality of the wear estimate. Indeed, running-in stage in reality is a complicated period, with the process of fretting wear, oxide film is removing, new metallic contact surface is generated and the contact surface roughed due to fretting wear.

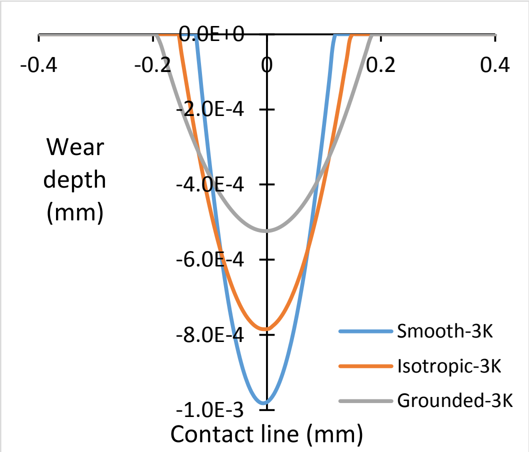

(a) F = 185 N

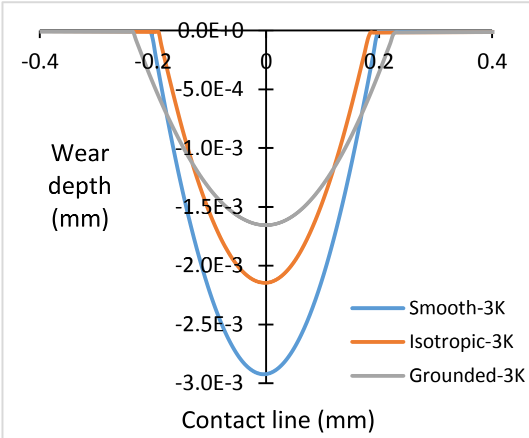

(b) F = 500 N

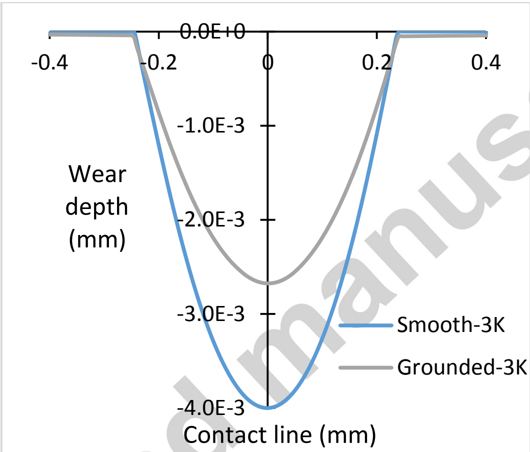

(c) F = 500 N

Figure 13. Wear scar predicted after 3000 cycles

Table 5. Wear volume [$\times 10^{-3} mm^3/mm$]

F [N]	Smooth-3K	Isotropic-3K	Grounded-3K
185	0.156	0.156	0.129
500	0.771	0.540	0.510
1670	1.262	-	0.88

The wear scars predicted by FE fretting wear model with different roughness, after 18000 cycles, are illustrated in Figure 14. In all three normal loading cases, the difference on wear scar among the cases of smooth surface, isotropic surface and grounded surface is limited. From numerical modelling point of view, it is because the effects of roughness are only considered in the first 3000 cycles by assuming the asperities of contact surfaces are worn out during this running-in stage. This assumption is confirmed by the work of [22], of which rough surface is considered directly into the fretting wear model.

Meanwhile, our results also point out that the influence of roughness of contact surface on wear scar is limited in gross sliding condition after 1800 cycles. This results are in agreement with experimental observation of fretting wear on steel conducted in [38], where tests showed the same tendency that the roughness has little influence on the wear scar in the gross sliding condition. Kubiak et al. [7] also showed results of fretting wear scars for three different initial roughness surfaces and there was no significant difference on the wear depths after test of all samples. These results suggest that the roughness effect on the fretting wear scar is negligible and a reduction on roughness does not seem to reduce the wear damage under gross sliding conditions.

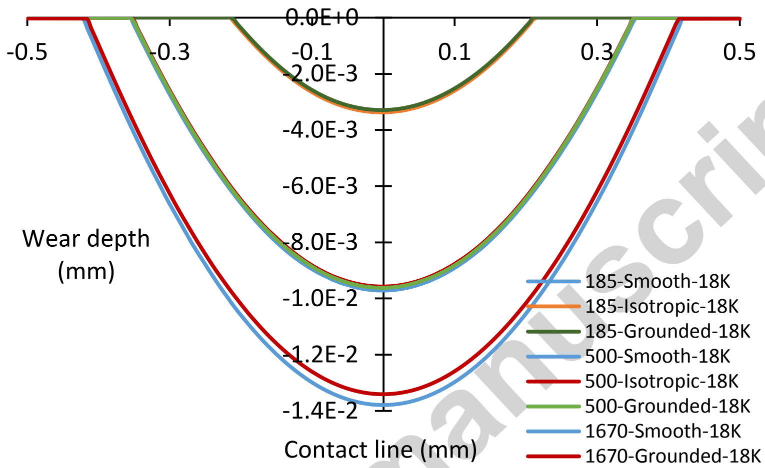

Figure 14. Fretting wear scar after 18000 cycles under different normal load cases, (a) F = 185 N, (b) F = 500 N, (c) F = 1670 N

5 Conclusion

In this paper we presented a multiscale methodology to consider the roughness effect in fretting wear simulations. In order to do that, we first analysed micro models to check the influence of roughness in the contact pressure distribution. Later, we studied the fretting problem in a macro scale, estimating the fretting wear scar evolution as function of the number of cycles. Finally, we considered the effect of roughness in fretting wear simulations, connecting the results from the small scale models to the large scale model. As supported by other research findings, our results also showed that roughness has a minor effect in the normal load under fretting wear in gross sliding condition.

Acknowledgment

The second author would like to acknowledge the research funding from China Scholarship Council.

References

[1] Rohatgi PK, Tabandeh-Khorshid M, Omrani E, Lovell MR and Menezes PL 2013 Tribology for Scientists and Engineers *Tribology for Scientists and Engineers: From Basics to Advanced Concepts* 233-268

[2] Yue T and Abdel Wahab M 2017 Finite element analysis of fretting wear under variable coefficient of friction and different contact regimes *Tribology International* **107** 274-282

[3] Yue T and Abdel Wahab M 2016 A numerical study on the effect of debris layer on frettingwear *Materials* **9** 597; doi:510.3390/ma9070597

[4] Singh R, Melkote SN and Hashimoto F 2005 Frictional response of precision finished surfaces in pure sliding *Wear* **258** 1500-1509

[5] Popov VL 2010 Contact mechanics and friction: physical principles and applications *Springer Science & Business Media*

[6] Kubiak KJ and Mathia TG 2009 Influence of roughness on contact interface in fretting under dry and boundary lubricated sliding regimes *Wear* **267** 315-321

[7] Kubiak KJ, Liskiewicz TW and Mathia TG 2011 Surface morphology in engineering applications: Influence of roughness on sliding and wear in dry fretting *Tribology International* **44**(11) 1427-1432

[8] Kubiak KJ, Mathia TG and Fouvry S 2010 Interface roughness effect on friction map under fretting contact conditions *Tribology International* **43** 1500-1507

[9] Raeymaekers B and Talke FE 2010 The effect of laser polishing on fretting wear between a hemisphere and a flat plate *Wear* **269** 416-423

[10] Yoon Y, Etsion I and Talke FE 2011 The evolution of fretting wear in a micro-spherical contact *Wear* **270** 567-575

[11] Bhatti NA and Wahab MA 2017 Finite element analysis of fretting fatigue under out of phase loading conditions *Tribology International* **109** 552-562

[12] Kumar D, Biswas R, Poh LH and Abdel Wahab M 2017 Fretting fatigue stress analysis in heterogeneous material using direct numerical simulations in solid mechanics *Tribology International* **109** 124-132

[13] Resende Pereira KdF, Bordas S, Tomar S, Trobec R, Depolli M, Kosec G and Abdel Wahab M 2016 On the Convergence of Stresses in Fretting Fatigue *Materials* **9** 639; doi:610.3390/ma9080639

[14] Ferjaoui A, Yue T, Abdel Wahab M and Hojjati-Talemi R 2015 Prediction of fretting fatigue crack initiation in double lap bolted joint *International Journal of Fatigue* **73** 66-76

[15] Hojjati Talemi R, Abdel Wahab M and De Baets P 2014 Finite element simulation of phase difference effects on fretting fatigue crack nucleation behaviour *Proceedings of the Institution of Mechanical Engineers Part J-Journal of Engineering Tribology* **228**(4) 470-479

[16] Hojjati Talemi R, Abdel Wahab M, Giner E and Sabsabi M 2013 Numerical estimation of fretting fatigue lifetime using damage and fracture mechanics *Tribology Letters* **52**(1) 11-25

[17] Hojjati Talemi R and Abdel Wahab M 2013 Fretting fatigue crack initiation lifetime predictor tool: using damage mechanics approach *Tribology International* **60** 176-186

[18] Yue T and Abdel Wahab M 2014 Finite element analysis of stress singularity in partial slip and gross sliding regimes in fretting wear *Wear* **321** 53-63

[19] McColl IR, Ding J and Leen SB 2004 Finite element simulation and experimental validation of fretting wear *Wear* **256** 1114-1127

[20] Paulin C, Fouvry S and Meunier C 2008 Finite element modelling of fretting wear surface evolution: Application to a Ti–6A1–4V contact *Wear* **264** 26-36

[21] Kasarekar AT, Bolander NW, Sadeghi F and Tseregounis S 2007 Modeling of fretting wear evolution in rough circular contacts in partial slip *International Journal of Mechanical Sciences* **49** 690-703

[22] Leonard DB, Sadeghi F, Shinde S and Mittelbach M 2013 Rough surface and damage mechanics wear modeling using the combined finite-discrete element method *Wear* **305** 312-321

[23] Aboudi J, Arnold SM and Bednarcyk BA 2013 Micromechanics of composite materials: a generalized multiscale analysis approach ed editors. Elsevier 984 p

[24] Anciaux G and Molinari JF 2010 Sliding of rough surfaces and energy dissipation with a 3D multiscale approach *International Journal for Numerical Methods in Engineering* **83** 1255-1271

[25] Anciaux G and Molinari J-F 2009 Contact mechanics at the nanoscale, a 3D multiscale approach *International Journal for Numerical Methods in Engineering* **79** 1041-1067

[26] Luan BQ, Hyun S, Molinari JF, Bernstein N and Robbins MO 2006 Multiscale modeling of two-dimensional contacts *Physical Review E - Statistical, Nonlinear, and Soft Matter Physics* **74** 1-11

[27] Stupkiewicz S, Lewandowski MJ and Lengiewicz J 2014 Micromechanical analysis of friction anisotropy in rough elastic contacts *International Journal of Solids and Structures* **51** 3931-3943

[28] Temizer İ and Wriggers P 2010 Inelastic analysis of granular interfaces via computational contact homogenization *International Journal for Numerical Methods in Engineering* **84** 883-915

[29] Temizer İ 2014 Computational homogenization of soft matter friction: Isogeometric framework and elastic boundary layers *International Journal for Numerical Methods in Engineering* **100** 953-981

[30] Jerier JF and Molinari JF 2012 Normal contact between rough surfaces by the Discrete Element Method *Tribology International* **47** 1-8

[31] Naylor T 1966 Computer simulation techniques ed editors. New York Wiley

[32] Hu YZ and Tonder K 1992 Simulation of 3-D random rough surface by 2-D digital filter and fourier analysis *International Journal of Machine Tools and Manufacture* **32** 83-90

[33] Johnson KL 1987 Contact mechanics ed editors. Cambridge university press

[34] Gentle JE 2012 Handbook of Computational Statistics Härdle WK, Mori Y ed editors. Berlin, Heidelberg Springer Berlin Heidelberg

[35] Milestone WD and Janeczko JT 1971 Friction between steel surfaces during fretting *Wear* **18** 29-40

[36] Greenwood JA and Tripp JH 1967 The Elastic Contact of Rough Spheres *Journal of Applied Mechanics* **34** 153

[37] Hisakado T, Miyazaki K, Kameta A and Negishi S 2000 Effects of surface roughness of roll metal pins on their friction and wear characteristics *Wear* **239**(1) 69-76

[38] Shi X 2001 Effect of the roughness of surface on fretting *MACHINERY* (05) 28-30

Highlights

- Multiscale procedure to study roughness effect on fretting wear using FE models.
- Micro scale model to analyse the effect of roughness on contact pressure
- A cylinder on plane contact configuration
- Roughness has a minor effect in gross sliding condition